

# Precise Distribution Simulation of Scattered Submunitions Based on Flight Test Data

**Sangyong Yun\* and Junsik Hwang\*\***

*Agency for Defense Development, 111, Sunam-dong, Yuseong-gu, Daejeon 34060, Republic of Korea*

**Jinyoung Suk\*\*\***

*Chungnam National University, Department of Aerospace Engineering, 99 Daehak-ro Yuseong, Daejeon 34134, Republic of Korea*

## Abstract

This paper presents a distribution simulation model for dual purpose improved conventional munitions based on flight test data. A systematic procedure for designing a dispersion simulation model is proposed. A new accumulated broken line graph was suggested for designing the distribution shape. In the process of verification and simulation for the distribution simulation model, verification was performed by first comparing data with firing test results, and an application simulation was then conducted. The Monte Carlo method was used in the simulations, which reflected the relationship between ejection conditions and real distribution data. Before establishing the simulation algorithm, the dominant ejection parameter of the submunitions was examined. The relationships between ejection conditions and distribution results were investigated. Five key distribution parameters were analyzed with respect to the ejection conditions. They reflect the characteristics of clustered particle dynamics and aerodynamics.

**Key words:** submunition, distribution, simulation, ejection

## Nomenclature

$C_D$	: Drag Coefficient [-]
$I_x$	: Axis Inertial Moment of Ammunition [kg-m <sup>2</sup> ]
$U$	: Relative Velocity ( $U = V - W$ ) [m/sec]
$V$	: Absolute Velocity [m/sec]
$W$	: Wind Velocity [m/sec]
$a$	: Pattern Diameter or Pattern Width of Cross Range Direction [m]
$b$	: Pattern Diameter or Pattern Width of Down Range Direction [m]
$d$	: Diameter of Submunition ( $= D_{REF}$ ) [m]
$g$	: Gravitational Acceleration [m/sec <sup>2</sup> ]
$m$	: Weight of Ammunition [kg]
$x$	: x Axis Coordinates [m]
$y$	: y Axis Coordinates [m]
$z$	: z Axis Coordinates [m]

## Greek Letters

$A$	: Coriolis' Angular Acceleration [m/sec <sup>2</sup> ]
$\emptyset$	: Yaw Angle [rad]
$\psi$	: Angle of Circumferential Direction [rad]
$\theta$	: Angle between Projectile or Missile and the Surface [rad]
$\rho$	: Air Density in the Atmosphere [kg/m <sup>3</sup> ]

## Subscripts

$B$	: Back
$D$	: Drag
$HOB$	: Height-of-Burst
$S$	: Submunition
$c$	: Centrifugal
$r$	: Radial

This is an Open Access article distributed under the terms of the Creative Commons Attribution Non-Commercial License (<http://creativecommons.org/licenses/by-nc/3.0/>) which permits unrestricted non-commercial use, distribution, and reproduction in any medium, provided the original work is properly cited.

© \* Principal Researcher: ysyong@add.re.kr  
\*\* Principal Researcher: hwangjs@add.re.kr  
\*\*\* Professor, Corresponding author: jsuk@cnu.ac.kr

## 1. Introduction

Possessing information regarding the distribution of some submunitions as determined from the ejection conditions is very essential. This is true from both operational and humanitarian viewpoints. In particular, users of cluster munitions should reduce the collateral damage caused to civilians; therefore, the user should recognize some distribution information regarding the cluster munition before firing.

James W. Purvis developed an automated collision model for use in submunition dispersion simulations [1]. A collision model was presented for use in digital computer simulations of submunition dispersion, and exact analytical equations were derived for the exchange of linear and angular momentum during a collision. Kristofer Peterson simulated the dispersion of several submunitions to evaluate weapon delivery probability parameters that included the circular error probability, range and deflection error probability, and weapon effectiveness of single and salvo weapons [2]. James E. Brunk presented a Monte Carlo analysis, introduced dispersion characteristics of some submunitions, and established the statistical input data required for a Monte Carlo analysis [3, 4]. Brunk studied another paper and presented self-dispersing bomblets that utilized passive control of the radial orientation of the trimmed lift force. The motions of these bomblets were determined from simplified theory and from exact six-degrees-of-freedom simulation. Brunk studied impact pattern predictions using the Monte Carlo method and showed that a properly designed S-curve and roll through zero bomblets can achieve large uniform patterns for low-altitude high-speed delivery conditions [5, 6]. Raymond Sedney introduced an ejection model of submunitions from missiles [7]. Sedney stated that when a submunition is penetrating a shear layer around a warhead, it is crucial as it may be trapped in a separated flow pocket. Results from the model are consistent with some observations and have been useful in studies. The aerodynamic interference phenomena of submunitions in the ejection phase have also been studied extensively [8, 9, 10, 11].

Most of the above papers are concerned with the distribution results, and trajectory simulations have been studied extensively and deeply with most of the above papers dealing with the ejection phenomena and offering theoretical and useful information. However, those papers do not involve real test results. This paper presents the design of a distribution simulation method that is matched with real flight test results based on a notion of the deep relationship between the aerodynamic interference phenomena and real

distribution results. The Monte Carlo simulation algorithm was used to accommodate the uncertainty in the real field data, which reflects the relationship between ejection conditions and distribution test data. The modified point mass trajectory equation of a DPICM projectile was used for the simulation. A fourth-order Runge-Kutta integration method was used. In the process of the trajectory calculation. Before establishing the simulation algorithm, the dominant ejection parameter of the submunition was examined, and the relationships between the ejection conditions and the distribution results were investigated in the application simulation. Ballistics and distribution characteristics were introduced for the analysis on the correlations between ejection conditions.

Some ejection phenomena of cluster submunitions from projectiles or missile warheads are examined in section 2. Section 3 describes the Monte Carlo simulation method using the equation of motion of a submunition combined with the initial velocity calculation equation of each submunition in the ejection phase. In section 4, an algorithm that matches simulation results with flight test results is presented with equations of motion. Section 5 describes the verification and simulation along with a detailed analysis. Finally, the conclusions of this study are presented.

## 2. Distribution and Ejection of Submunitions

### 2.1 Ejection Phenomena of Cluster Submunitions

The size and pattern of the distribution depends on the aerodynamic characteristics, mass properties of the submunition, ejection velocity, ejection mechanism, warhead dive angle, air density, wind speed, etc.

Figure 1 shows the structure of Dual Purpose Improved Conventional Munition (DPICM) type submunition used for anti-personnel and anti-armor purposes [21]. Fig. 2 shows the ejection scene of DPICM submunitions from a 155 mm artillery projectile [21].

When submunitions are ejected from a warhead, they

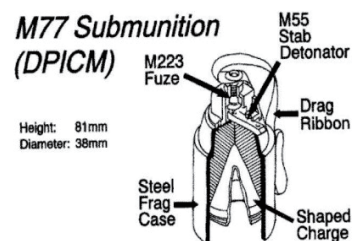


Fig. 1. Structure of M77 DPICM submunition.

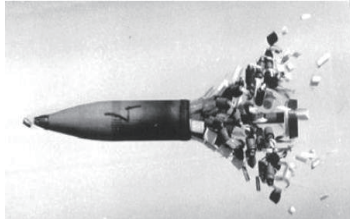


Fig. 2. Ejection scene of DPICM submunitions from a projectile.

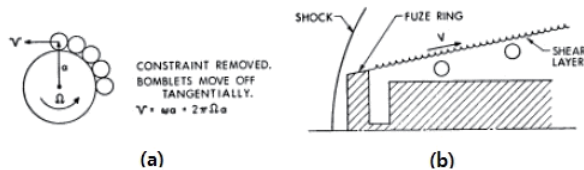


Fig. 3. Shock and vortex sheet around a warhead.

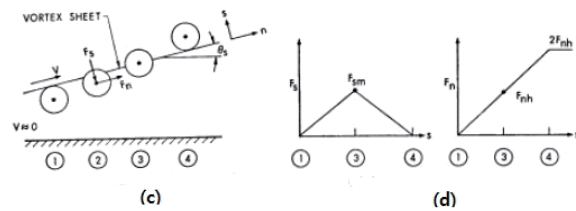
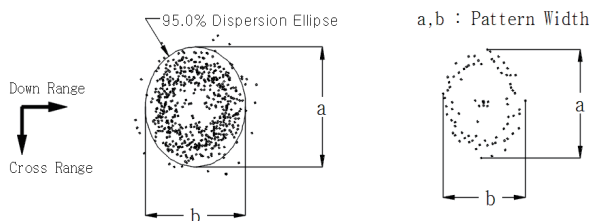


Fig. 4. Interference degree of a vortex sheet according to the position of a submunition.

pass through a complicated flow field in a short period of time. The dispersion pattern and sizes of submunitions can be determined from the aerodynamics and physical characteristics of the submunition, the warhead dispenser system, the ejection conditions, and the atmospheric conditions. Figs. 3 and 4 describe the effect of the shock and vortex sheet around the warhead during the ejection of submunitions [7].

## 2.2 Distribution of Submunitions

The distribution pattern of submunitions generally exhibits an elliptic form. In general, the pattern diameter in the cross-range direction is "*a*" and that in the down-range direction is "*b*", as shown in Fig. 5. In some cases, "*a*" and "*b*" indicate the pattern width of the cross-range and the

Fig. 5. Definition of pattern diameter *a* and *b*.

down-range directions, respectively. The distribution size of the submunition is expressed as an ellipse that contains 95% or 97.5% of the dispersed submunitions. A typical dispersion size is a 95% ellipse. In some cases, "*a*" and "*b*" then indicate the major and minor pattern diameters, respectively. The average pattern diameter is expressed as like. In this paper, is used as the average diameter.

## 3. Ejection Algorithm and Equations of Motion

### 3.1 Ejection Model of the Cluster Submunition Using the Monte Carlo Method

Here, the test result is represented by the distribution coordinate value of the DPICM submunition. When selecting suitable data from numerical coordinate data or photographs of the distribution of submunitions after a flight firing test, the most important thing is to select data that have a pattern ratio (*b/a*) value close to 1.0. If we obtain data with a *b/a* value of less than 1.0, we have to modify the ratio up to 1.0 and then measure the coordinate value. If there is no numerical coordinate data or photographs of a new submunition, we can use the coordinate data or photographs of a similar submunition. However, after a firing test, the distribution information must be substituted with new information.

We studied the dispersion pattern of DPICM submunitions by varying the ejection velocity, mass, and drag coefficient using the Monte Carlo simulation method.

Subroutine "RAN0 (IDUM)" generates a random number evenly from 0 to 1. The random number generator was supplied from a related book [15]. When we generate random numbers 100 times, the number of distributed values should be even for all subintervals. If we use the random number generator in this way and throw a ball from 0 to 50 meters, it will be distributed evenly and produce the histogram shown in Fig. 6. Here the balls' weights, external dimensions, ejection angles, and the values of gravitational acceleration are assumed to be the same. The atmosphere is also assumed to be a vacuum. However, it is not realistic.

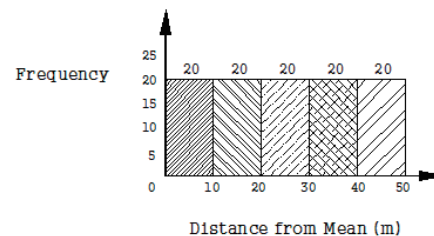


Fig. 6. Histogram obtained from a random number generator.

Let us assume that we have some ball throwing machine that produces the histogram shown in Fig. 7. As carried out for Fig. 6, if we use a random number generator for values between 0 and 1 and if we want a distribution like that in Fig. 7, the frequency must be identified preferentially according to the section. For the generation of 100 random numbers, there should be a distribution of 5 times between the interval of 0 and 10, 10 times between the interval of 10 and 20, 15 times for 20 and 30, 25 times for 30 and 40, and 45 times for 40 and 50.

Next, we will mark the number of events for each interval from the 100 specimens and produce a histogram as an accumulated histogram, as shown in Fig. 8. Then, the

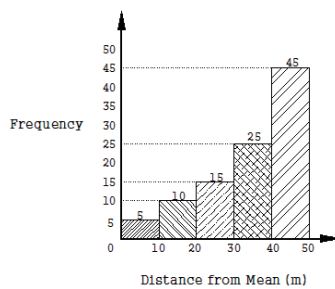


Fig. 7. Histogram obtained from assumptions.

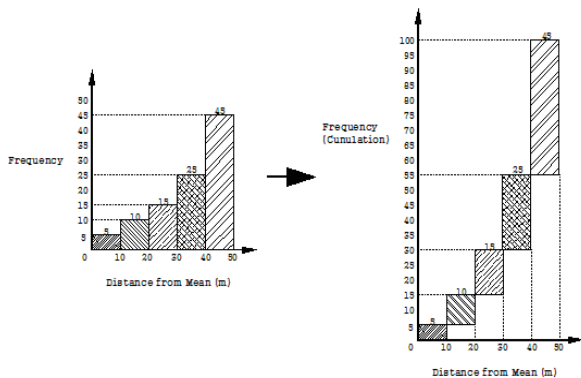


Fig. 8. Changing to an accumulated histogram

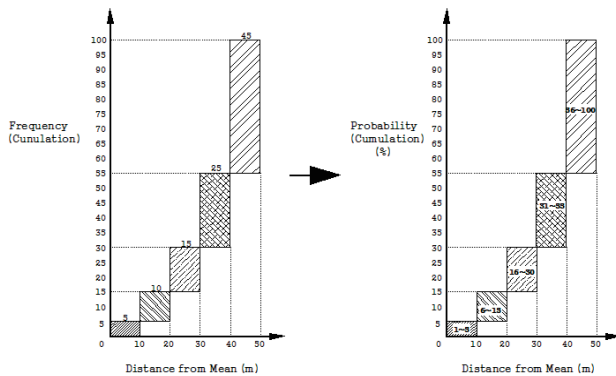


Fig. 9. Normalized y axis.

distribution probability of each interval can be obtained by changing as shown in Fig. 9 with the normalization of the y axis. Then, a normalized x axis is obtained by dividing the section value by the maximum distance as shown in Fig 10. Finally, we can produce a new broken curved graph. A new random number can be calculated between 0 and 1 in the new curve as shown in Fig. 11.

Figure 11 shows the one to one matching between the random number,  $RAN0(J)$ , generated from the external function in the program and another random number,  $RAND(J)$ .  $RAND(J)$  is used for the multiplication with the maximum ejection speed. If the maximum speed is 50 m/s, the random speed will be located between 0 and 50 m/s and follow the frequency distribution shown in Fig. 7. Fig. 12 shows the program flow chart used in this study. The calculations were carried out in the order from the first submunition to the last ( $N^{th}$ ) submunition. The behavior of an individual submunition was calculated from the ejection time to the impact time for each time increment with input values of the initial condition such as HOB, velocity, atmospheric state, aerodynamic coefficients, etc.

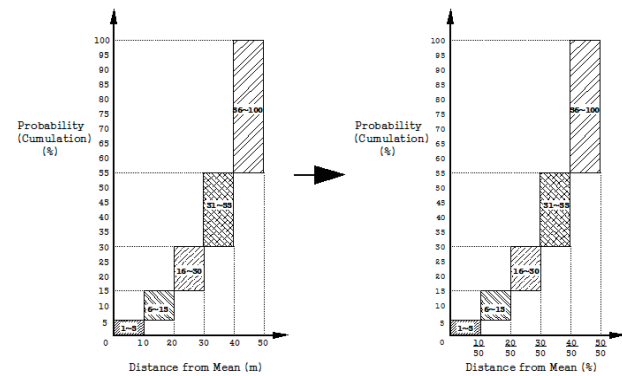


Fig. 10. Normalized x axis.

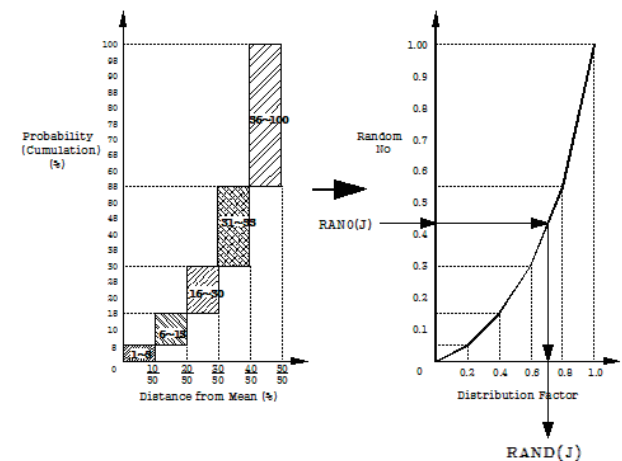


Fig. 11. The change from a histogram to broken curved graph.

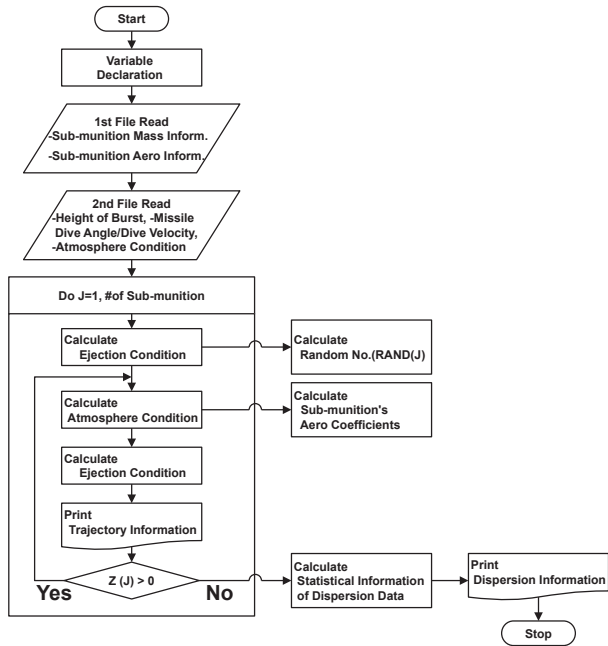


Fig. 12. A flowchart of the dispersion simulation.

## 3.2 Trajectory Analysis Model of Submunitions

### 3.2.1 Assumptions

Except for f, the assumptions used in this paper are based on the standard conditions of a firing table.

- The climate is calm.
- The altitude of the impact region is sea level.
- The Earth is flat.
- The impact pattern differs according to the dispensing system of the warhead and the aerodynamic and physical characteristics of the submunition.
- Submunitions are ejected with a uniform angular distance and fall in the radial direction.
- The distance from the ejection point to the impact point is proportional to the dominant ejection parameter.

### 3.2.2 Coordinate System

The coordinate system used here to display the trajectory

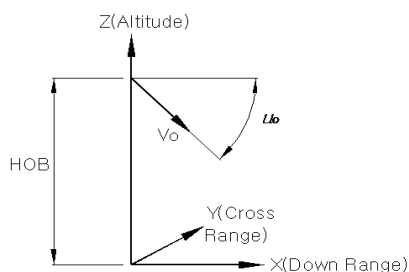


Fig. 13. Coordinate system of the trajectory simulation of submunitions.

motion equations of submunitions is a ground-fixed Cartesian coordinate system, as shown in Fig. 13.

### 3.2.3 Trajectory Motion Equations

Figure 14 shows a schematic diagram of the ejection of DPICM submunitions for explaining the ejection equations. The longitudinal velocity  $V_{HOB}$  of cluster submunitions at HOB is the sum of the velocity of the carrier projectile  $U_{HOB}$  and the ejection velocity  $\Delta U$ ,

$$V_{HOB} = U_{HOB} - \Delta U \quad (1)$$

If  $\Delta U$  is zero,  $V_{HOB}$  is equal to  $U_{HOB}$ ,

$$V_S = \sqrt{V_c^2 + V_r^2} \quad (2)$$

The ejection velocity  $V_S$  is a candidate for the dominant ejection parameter, and consists of the circumferential ejection velocity  $V_c$ , the centrifugal force, and the radial velocity  $V_r$ . When the carrier projectile has a spin, there is a circumferential ejection velocity. If the carrier projectile's spin velocity is zero, then  $V_S$  is equal to  $V_c$ .

Here, let us assume that the warhead of the carrier projectile has  $N$  submunitions, and that the ejection velocity  $V_S$  varies at HOB. The trajectory simulation of submunitions must be carried out from the 1<sup>st</sup> submunition to the  $N^{\text{th}}$  submunition. The following equations (3), (4), and (5) are motion equations of the  $j^{\text{th}}$  submunition. The distributed random number  $\text{RAND}(j)$  in the second term of the right hand side of these equations were calculated in the ejection model for Monte Carlo simulations in the ground-fixed coordinate system.

$$U_x(j) = U_{xHOB} - (\sin\theta \cos\phi_s + \sin\theta \cos\phi \cos\psi_s)[V_S \times \text{RAND}(j)] \quad (3)$$

$$U_y(j) = U_{yHOB} + (\cos\theta \cos\phi_s - \sin\theta \cos\phi \cos\psi_s)[V_S \times \text{RAND}(j)] \quad (4)$$

$$U_z(j) = U_{zHOB} + (\cos\theta \sin\psi_s)[V_S \times \text{RAND}(j)] \quad (5)$$

The trajectory equation used in this study was the point mass trajectory equation [12, 13]:

$$d\frac{\bar{U}}{dt} = -\frac{\pi\rho d^2 V \bar{V}}{8m} C_D + \bar{g} + \bar{A} \quad (6)$$

The first term of the right hand side of equation (6) is the acceleration due to air drag. The second term is gravitational acceleration, and the third term is Coriolis' acceleration.

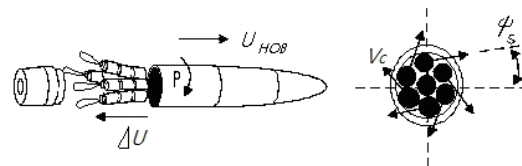


Fig. 14. A schematic diagram of the ejection of submunitions.

Here, let us consider another candidate for the dominant parameter: the variation of mass  $m$  in equation (6). The following equation (7) is the trajectory equation of the  $j^{th}$  submunition for determining the effect of mass variations.

$$d \frac{\bar{V}}{dt} = - \frac{\pi \rho d^2 V \bar{V}}{8 [m \times \text{RAND}(j)]} C_D + \bar{g} + \bar{A} \quad (7)$$

Another candidate for the dominant parameter is the variation of the drag coefficient  $C_D$  in equation (6). The following equation (8) is the trajectory equation of the  $j^{th}$  submunition for determining the effect due to variations in the drag coefficient.

$$d \frac{\bar{V}}{dt} = - \frac{\pi \rho d^2 V \bar{V}}{8 m} [C_D \times \text{RAND}(j)] + \bar{g} + \bar{A} \quad (8)$$

When variations in the mass or drag coefficient are used, the distributed random number  $\text{RAND}(j)$  of equations (3), (4), and (5) are omitted.

## 4. Numerical Simulation

To carry out a verification of the trajectory simulation model, we first compared data with DPICM projectile firing test results, and repeated simulations were then carried out. The aerodynamic data of the projectile and submunition used in the simulation model were supplied from the aerodynamic data for the firing table.

### 4.1 Preliminary Verification

The firing table contains information such as the muzzle velocity, range, drift, etc. Code for the firing table is needed to determine the aerodynamics of the package, physical properties of the carrier projectile and its submunitions, firing velocity, etc. [16, 17]. Fig. 15 shows the trajectory simulation results for a DPICM projectile obtained using the modified point mass trajectory equation [13]. Fig. 16 shows the results from a DPICM projectile flight test that clearly describes the scattered position of the individual submunitions. A simulation model was constructed using

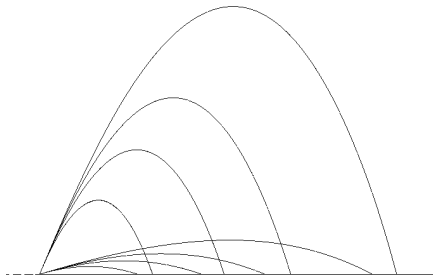


Fig. 15. Trajectory simulation results of a DPICM projectile.

this distribution data.

To obtain a submunition ejection model, a histogram was generated as shown in Fig. 17 from Fig. 16. After a distributed random number  $\text{RAND}(j)$  was obtained from the histogram, it was used as input data by multiplying it with the ejection parameters. The ejection parameters are the mass information  $m(j)$ , the drag coefficient  $C_D(j)$ , and the ejection velocity  $V_s(j)$ . The variation limits of mass, drag coefficient, and ejection velocity are considered sufficiently, for example, the sufficient variation limit of the mass was within 5%. Fig. 18 illustrates several simulation results of DPICM submunitions determined using the distribution simulation model with the information in the histogram shown in Fig. 17. As shown in Fig. 18, the simulation results in case (d) resembles the shape and dimensions shown in Fig. 16. The effect of variations in the mass and the drag coefficients of the submunitions were small. Therefore, we concluded that the dominant parameter that determines the shape and dimensions of the distribution is the ejection at HOB. Fig. 19 shows the 3 dimensional trajectories of several submunitions from HOB to the impact area with variations in the ejection velocity. Table 1 shows a summary of the test results for Fig. 16 and the simulation results in Fig. 18(d). The maximum and minimum distances that are shown in Table 1 are the distances from the mean impact point. As shown in Table 1, in the case of the outer distribution, the values of the

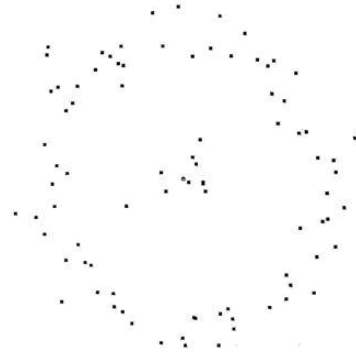


Fig. 16. Firing test results of a DPICM projectile.

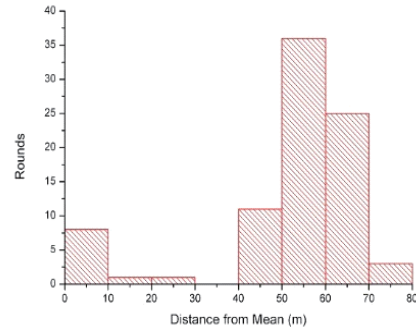


Fig. 17. Histogram obtained from test results of DPICM submunitions.

simulation results are somewhat lower than those of the test data, while the pattern width ratio  $b/a$  is very similar to that of the test results. In the case of the inner distribution, the values of the simulation results are somewhat less than those of real flight test data. The deviation of the pattern dimensions  $a$  and  $b$  between the simulation and real flight test data was less than 2%. Furthermore, the dispersion pattern ratio agrees well with the test results. The differences between the

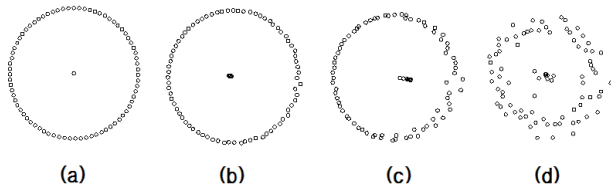


Fig. 18. Several dispersion cases with variations in mass, drag coefficient, and ejection velocity of DPICM submunition. (Inner: 10 rounds, outer: 75 rounds).

- (a) No variation in mass, drag coefficient, and ejection velocity of the submunitions.
- (b) Variation in mass of the submunition of within 5% during flight.
- (c) Variation in drag coefficient of the submunition of within 20% during flight.
- (d) Variation in the ejection velocity of the submunition at height-of-burst.

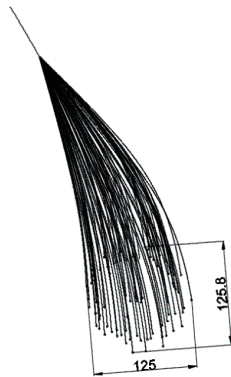


Fig. 19. Trajectory simulation diagram of DPICM submunitions.

simulation and test results are due to the incompleteness of simulation algorithms, unsuitable assumptions, differences in the atmospheric state, measurement errors, etc. Regardless, the results of the distribution simulation model agree relatively well with the test results.

## 4.2 Application Simulation

To simulate another distribution, some information is needed. However, if there is no information regarding the cluster weapon, one can assume the distribution information as shown in Fig. 20. We can also assume the specifications of the submunitions and the ejection conditions. As in the above verification, a distribution simulation model must be constructed. Fig. 21 shows a distribution chart using the ejection modeling algorithm proposed in this study. Now, we can simulate some conditions. If there is no information about the initial simulation conditions, we can also assume those shown in Table 2. If there is detailed information about a specific weapon, that can be used instead. Fig. 22 shows the simulation results with a 3 dimensional point of view.

The analysis was executed qualitatively rather than quantitatively because most of the simulation conditions

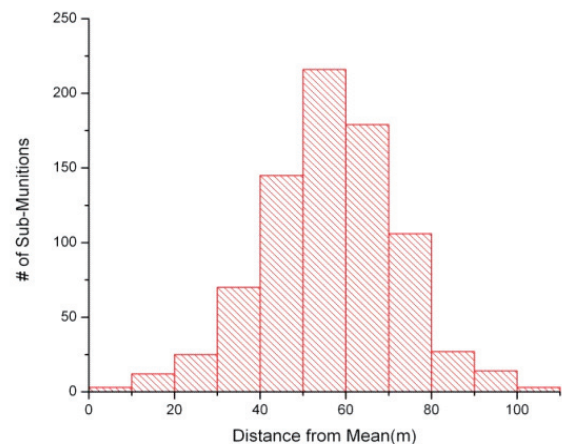


Fig. 20. Simulation histogram.

Table 1. Comparison between test and simulation results.

	Outer Distribution (75 Submunitions)					Inner Distribution (10 Submunitions)	
	Maximum	Minimum	Pattern Width			Maximum	Minimum
	Distance (m)	Distance (m)	$a$ (m)	$b$ (m)	$b/a(-)$	Distance (m)	Distance (m)
Flight Test	69.8	39.7	123.5	124.6	1.01	23.4	2.5
Simulation	67.5	37.6	125.8	125.0	0.99	21.2	2.6
Difference	-2.3	-2.1	+2.3 (+1.9%)	+0.4 (+0.3%)	-0.02	-2.2	+0.1

were based on assumptions. The analyzed results for determining the correlations among the ejection conditions, ballistics, and distribution characteristics are as follows.

As shown in Fig. 23, in the case of an average pattern diameter ratio, when the ejection angle is close to the vertical direction, the result is close to the value of 1.0 regardless of the ejection altitude. This exhibits the tendency of having a value larger than 1.0 when the ejection altitude decreases

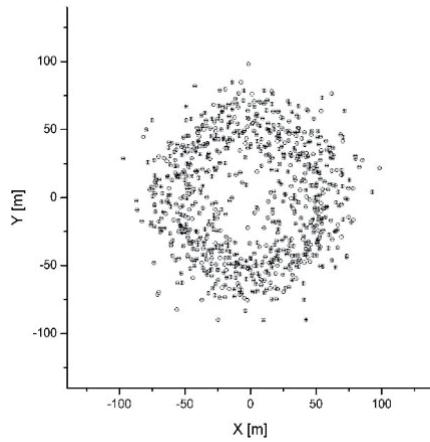


Fig. 21. Simulation distribution chart.

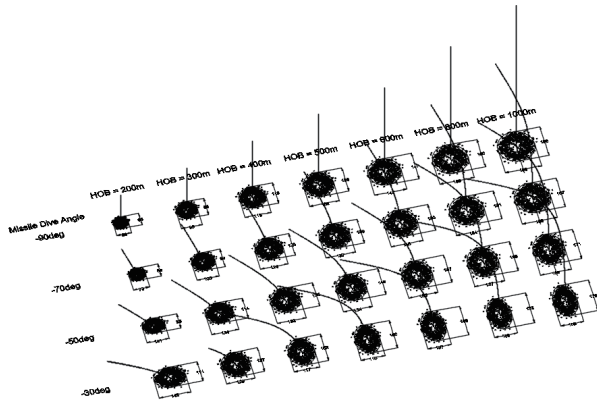


Fig. 22. Simulation distribution results.

Table 2. Simulation conditions.

	Condition	Remarks
Submunition	* Type : DPICM * Quantity Number : 800	
Maximum Ejection Velocity [m/s]	60	
Height-of-Burst [m]	①200 ②300 ③400 ④500 ⑤600 ⑥800 ⑦1000	
Missile Dive Angle [degree]	-90 ②-70 ③-50 ④-30	Here, Missile Dive Angle = Ejection Angle
Missile Velocity at HOB [m/s]	289 (Mach 0.85)	

and having a value less than 1.0 when the ejection altitude increases. Fig. 24 shows that the outer region's average pattern diameter increased with a high ejection altitude but had no relationship with the ejection angle. The increasing rate of the diameter dwindled when the ejection height was increased and the diameter variation was small at low ejection altitude conditions. At lower altitude conditions, the average pattern diameter increased with a low ejection angle value from the horizontal direction, while at higher altitude conditions, the average pattern diameter decreased with a low ejection angle value. As shown in Fig. 25, the average falling velocity of the ejected submunitions

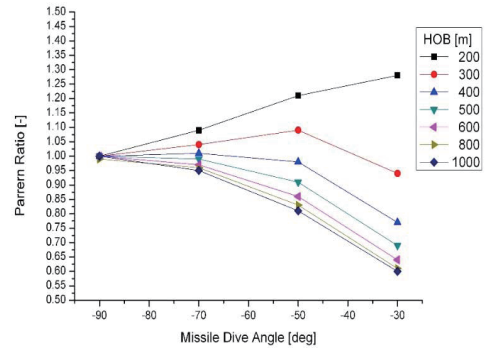


Fig. 23. The relationship between the pattern diameter and the missile dive angle.

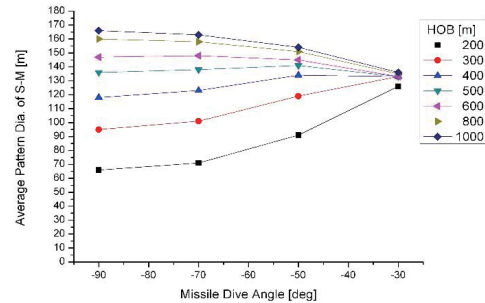


Fig. 24. The relationship between the average pattern diameter and the missile dive angle.

decreased with increasing ejection altitude and a low value of the ejection angle from the vertical direction. When the HOB is very high, the average falling velocity converges to a constant value. Fig. 26 shows that the average time of flight of the ejected submunition family increases with the altitude and a low angular value from the horizontal direction. Fig. 27 shows that the leading distance between the ejected submunitions increased with the altitude and a lower ejection angle. When the missile dive angle was close to the vertical direction, the leading distance was close to the value of 0 meters without regard to the ejection altitude. All of the above results validate the proper design consequences of the simulation modeling.

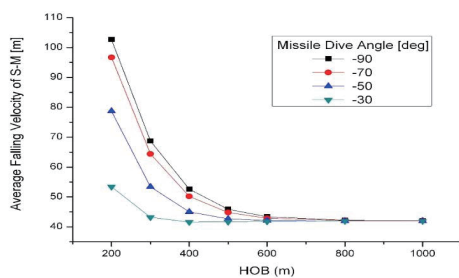


Fig. 25. The relationship between the average falling velocity and the height-of-burst.

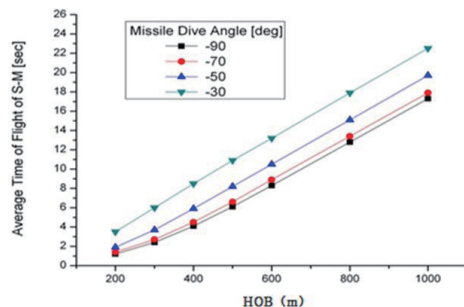


Fig. 26. The relationship between the average time-of-flight and the height-of-burst.

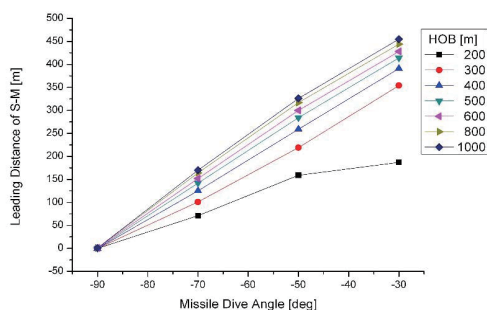


Fig. 27. The relationship between the leading distance\* and the missile dive angle.

\* Leading distance: the distance between HOB and the mean of submunitions in the x direction.

## 5. Conclusions

This paper deals with a distribution simulation model of submunitions from flight test data. Before establishing the simulation algorithm, the dominant ejection parameter of submunitions was examined.

In a preliminary verification, the simulation results agreed well with the flight test results. In application simulation using the model, relationships between the ejection conditions and the distribution results were investigated. It was also verified that the histogram design with respect to the dispersion distance has a close relationship with the distribution pattern and dimension. In particular, this paper proposed a new method that emancipates the entire distribution solution by introducing a normalized broken line graph from the accumulated histogram. Several numerical simulations were performed with respect to the ejection angle and the height-of-burst. As a result, five individual distribution characteristics (pattern diameter ratio, average pattern diameter, average falling velocity, average time-of-flight, and leading distance) were analyzed, all of which reflected the clustered particle dynamics and aerodynamics very well. All the results presented herein show that the proposed distribution simulation model can be used effectively to determine the optimal ejection conditions for Dual Purpose Improved Conventional Munitions.

## Acknowledgement

This work was supported by research fund of Chungnam National University.

## References

- [1] James, W. P., "Rigid Body Collision Model for Submunition Dispersion Simulation", *AIAA Journal*, Vol. 20, No. 3, 1983, pp. 195–200.
- [2] Kristofer, P., "Numerical Simulation Investigations in Weapon", *Naval Postgraduate School*, Monterey, California, 2008.
- [3] James, E. B., "Aerodynamic Dispersion Techniques", *US Air Force Armament Laboratory*, AFATL-TR-70-123, 1970.
- [4] James, E. B., "Aerodynamics and Flight Mechanics of Magnus-Rotor Bomblets", *US Air Force Armament Laboratory*, AFATL-TR-68-73, 1968.
- [5] James, E. B., "Monte Carlo Analysis of S-Curve and Roll-Through-Zero Bomblet Dispersion Characteristics", *US Air Force Armament Laboratory*, AFATL-TR-70-123, 1970.
- [6] James, E. B., "Flight Dynamics and Dispersion

Characteristics of S-Curve and Roll-Through-Zero Bomblets, *US Air Force Armament Laboratory*, AFATL-TR-72-171, 1972.

[7] Raymond, S., "A Model for Bomblet Ejection from Missiles," *AIAA Journal*, Vol. 24, No. 4, 1978, pp. 229-235.

[8] William, E. D., "Simulation and Analysis of Multiple Body Dispense Event," *AIAA Paper* 1252, 2004.

[9] Harris, L. E., Jubaraj, S. and Karen, R. H., "Computational Fluid Dynamics Modeling of Submunition Separation from Missile," *AIAA* 99-3129, 1999.

[10] David, A. C., Brien, E. E. and George, M. L., "Prediction of Submunition Dispense Aerodynamics," *AIAA Paper* 95-0331, 1995.

[11] Rayatistas, G. H., Lin, S. and Kwok, C. K., "Reverse Flow Radius in Vortex Chambers," *AIAA Journal*, Vol. 24, No. 11, 1986.

[12] Farrar, C. L. and Leeming, D. W., "Military Ballistics," *Royal Military College of Science*, Shrivenham, UK, 1982, Chap. 4.

[13] Robert, L. M., "Aero Ballistics," *BRL*, 1963, Chaps. 1, 2, 4.

[14] Melvin, J. M. and Robert, J. L., *Numerical Analysis*, 3<sup>rd</sup> ed., Wadsworth Publishing Company, California, 1991, pp.

447-449.

[15] Brian, P. F., Saul, A. T. and William, T. V., *Numerical Recipes*, Cambridge University Press, New York, 1989, pp. 191-199.

[16] FT 155-AN-1 Firing Table, Department of the Army Headquarters, 1976, Part 1.

[17] FT 155-AU-PAD Firing Tables, Ballistic Research Laboratory, 1989, Part 1.

[18] Lamar, M. A. and Dahlke, C. W., "Drag Characteristics of Ribbons," *16th AIAA Aerodynamic Decelerator Systems Technology Conference and Seminar*, Boston, MA. 2001.

[19] Lamar, M. A. and Brette, L. W., "Application of Fabric Ribbons for Drag and Stabilization," *18th AIAA Aerodynamic Decelerator Systems Technology Conference and Seminar*. Vol. 1618, 2005.

[20] Carruthers, F., "On the Aerodynamic Drag of Streamers and Flags," *AIAA Aerospace Sciences Meeting and Exhibit*, Reno, NV, January 2005.

[21] Ove D., "Cluster Weapons—Military Utility and Alternatives," *Norwegian Defense Research Establishment (FFI)*, 2008.